A&A, 711, A204 (2026)
https://doi.org/10.1051/0004-6361/202558813

Astronomy & Astrophysics

Asymptotic giant branch-stars in the GLIMPSE database

II. Distribution in the inner Milky Way

H. J. Habing[1,⋆] and M. A. Habing[2]

[1] Leiden Observatory, PO Box 9513, 2300 RA Leiden, The Netherlands
[2] Paltzerweg 38, 3722 JG Bilthoven, The Netherlands

Received 29 December 2025 / Accepted 28 May 2026

ABSTRACT

Aims. In the preceding paper (paper I) we showed that the GLIMPSE database contains millions of asymptotic giant branch (AGB) stars. Their nature follows from two properties: the objects have the same color after correction for interstellar extinction (see paper I, Fig. 7), and the number of objects grows exponentially with the apparent magnitude at 8 μm and always at the same rate; the growth in luminosity follows from the predicted exponential increase in luminosity of AGB stars (see paper I, Fig. 14).

Methods. We analyzed the interstellar extinction of the stars and the variation in their numbers as a function of longitude to derive their Galactic distribution and their association with interstellar dust.

Results. We find that the stars are spread out in a flat disk with a radius of about 7 kpc embedded in a presumably larger, flat, thick layer of dust. The counts of the stars led to the distinction of three populations of AGB stars: (i) an outer disk for $R > 1.5$ kpc with a density that rises slowly toward the Galactic Center (GC), (ii) an inner disk for $R < 1.5$ kpc with a stellar density that rises rapidly toward the GC ($\approx R^{-4}$) and (iii) inside $R = 300$ pc the GC Area that contains the Inner Galactic Bulge (IGB) and the Nuclear Stellar Disk (NSD). We present complete 2D images of both objects. Inside the NSD the dust density is significantly enhanced and the luminosity of the AGB stars is higher than elsewhere in the Milky Way. The NSD is the true center of the Milky Way.

Conclusions. The GLIMPSE database contains a full description of the AGB stars in the inner Milky Way.

Key words. astronomical databases: miscellaneous – stars: AGB and post-AGB – stars: variables: general

1. Introduction

The GLIMPSE database contains many millions of point sources (see paper I). In previous analyses of the database it was concluded that most of these point sources were either young stellar objects (YSOs) or asymptotic giant branch (AGB) stars and that their numbers were comparable. We disagreed and concluded that almost all the objects brighter than [8.0] = 12 are AGB stars.

To decide whether a point source is an AGB star or a YSO we use three arguments: first, there is a convincing difference in color [3.8] – [8.0] between YSOs and AGB stars after correction of the AGB stars for interstellar extinction (Fig. (1) in paper I). Second, the color $K-[8.0]$ of AGB stars has a very narrow distribution around 0.0 (see Fig. (7) in paper I). Third, in test fields for longitudes farther away than 10° from the Galactic Center (GC), the number of AGB stars increases exponentially with [8.0] and always at the same rate except at the brightest magnitudes (<5.0) and at the faintest (>11.0) (Figs. 14 and 15 in paper I). From the Spectral Energy Distribution (SED) we derived the bolometric magnitude, $m_{\rm bol}$; the interstellar extinction, Ak; and the optical depth of a circumstellar envelope, $\tau_{\rm CSE}$.

In this paper (paper II), we derived the distribution of the AGB stars in the inner Milky Way and especially around the Galactic Center (GC). In paper I we analyzed 31 fields of one square degree. In between the writing of papers I and II we enlarged the number of test fields from 31 to 49; 25 fields located at 5° distance between $l = -60°$ and $l = +60°$; and a chain of 31 adjacent fields from $l = -15°$ to $+15°$; excluding doubles the total number of fields is 49. The main reason for enlarging the number of test fields was to better study a potential asymmetry in the distribution in the Galactic plane that might have been caused by the Galactic bar. We did not find the bar as we discuss below.

As in paper I, we use $R_{GC} = 8.2$ kpc, or $m - M = 14.56$ (Reid et al. 2019).

Our analysis has profited from earlier discussions of the stars and dust properties in the GLIMPSE database: Benjamin et al. (2005), Robitaille et al. (2008), Churchwell et al. (2009), Robitaille et al. (2012) and Natale et al. (2022).

2. Galactic extinction

Interstellar extinction can be measured easily and reliably from the J and H magnitudes (Majewski et al. 2011). The measurement of Ak in so many stars distributed along the Galactic equator offers information about the distribution of dust and stars in the Milky Way. A determination of Ak requires the magnitudes in the J- and H-channels and when the extinction is large (e.g. $Ak > 2$ or $Av > 20$) the sensitivity of the 2MASS survey (which provided the J,H, and K magnitudes in the GLIMPSE database) was too low, and so Ak could not be determined. We studied diagrams of [8.0] versus J and concluded that for stars brighter than [8.0] = 8 the number of missing Ak measurements is below 10%. We therefore used only these brighter stars in our discussion of the dust distribution.

The quantity Ak is the integral of dust particles along the line of sight; its value grows monotonically with distance. Ideally, the

⋆ Corresponding author: martijnhabing@gmail.com

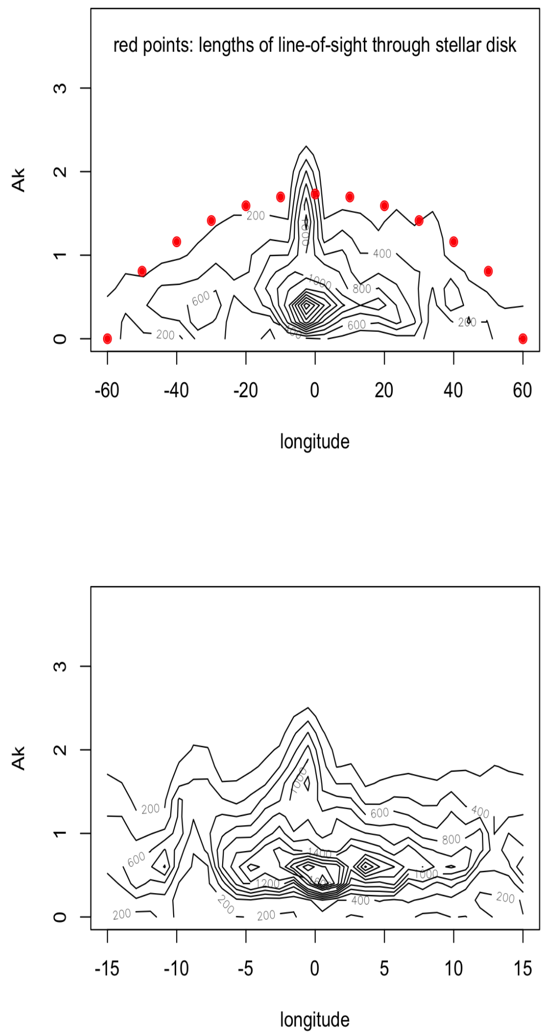

Fig. 1. Distribution of $n(Ak, l)$, the number of stars with $[8.0] \leq 8.0$ and with extinction Ak in a field of 1 square degree in the direction l. In the top diagram the fields are 5° apart; in the bottom diagram the fields are adjacent. The red dots are given by equation $n(Ak, l) = 1.8 \cdot \sqrt{(\sin 60)^2 - (\sin l)^2}$.

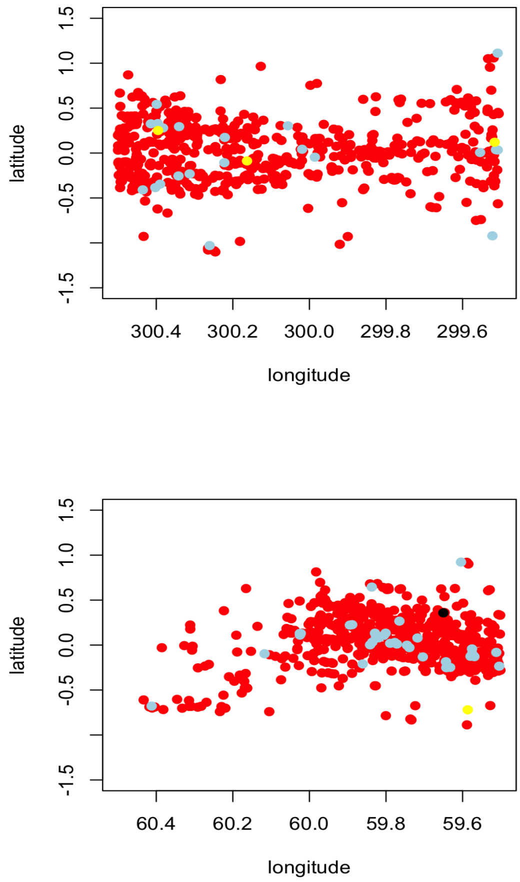

Fig. 2. A longitude-latitude plot of GLIMPSE stars in fields centered at $l = 60°$ and $l = 300°$. In the bottom diagram, 540 stars are red ($1.0 < Ak < 1.5$), 21 light blue ($1.5 < Ak < 2.0$), and 3 yellow ($2.0 < Ak < 2.5$). These numbers confirm that we are looking at the edge of the stellar disk. Similar numbers apply to the top diagram.

distance to a star can be derived from its Ak value but the detailed distributions of extinction in directions close to the GC by Zhang et al. (2025) and Vergely et al. (2022), reveal large and irregular variations in Ak with position. The distance determination to an individual star will be uncertain, but for large samples of stars the mean distance is, we expect, successful. A total extinction of $Ak = 1$ corresponds to $AV = 10$ and, when dust and gas are mixed in the usual ratio, $Ak = 1$ corresponds to an approximate surface density of $N(H_2) + N(H) = 2 \cdot 10^{22}$ cm^{-2} (Güver & Özel 2009).

The distribution of $n(Ak, l)$, the number of stars with extinction Ak in longitude direction l, is shown in Fig. 1 in two contour diagrams. In the top diagram the longitudes range from −60° to +60° in steps of 5° and in the bottom diagram the longitudes range from −15° to +15° in steps of 1°.

The top diagram shows modest structure except around the GC where there is some action; leave that area aside for a moment. In this diagram we noted the curvature in the contours. If we assume that the AGB stars form a circular disk around the GC with radius $R_{GC} \sin(60°)$ and that the dust is in a uniform disk with a total extinction $Ak = 1.8$ it follows that the total amount of dust along a line of sight in the direction equals $1.8 \cdot \sqrt{(\sin 60)^2 - (\sin l)^2}$ – see the red points. Near the GC there is extra extinction of about $Ak = 1.5$ that is produced at the distance of the GC. The agreement between this simple model and the observations is fair.

The model of the dust disk predicts that AGB stars disappear from sight at $|l| = 60°$. This is confirmed in Fig. 2, which shows (l, b) plots of stars in the directions $l = +60°$ and $-60°$. To see the disappearance of the disk compare the number of stars in Fig. 2 to that in Fig. 3, which shows the AGB disk at its best.

In paper I (Fig. 13 and conclusion 7), we decided that the end of the AGB disk is reached between magnitudes $[8.0] = 11$ and 12. This confirms the present statement that the GLIMPSE database detects AGB stars out to the limits of their distribution in the Milky Way.

The disk of stars is thus seen out to the longitude $l = \pm 60°$, but the dust disk extends farther. The layer of CO gas (see Figs. 6 and 7 in Dame et al. 2001) extends to at least $l = \pm 80°$ and where there is molecular gas there must be dust.

Now consider the diagrams in directions close to the GC. The bottom diagram in Fig. 1 is more detailed and shows a strong concentration of sources near $l = 0°$ without an increase in Ak. Above this concentration of stars around the GC, there is an outbreak in the contours to larger values of Ak and that reflects a disk of dust with a radius of 1° and total extinction of $Ak = 1.5$; around the GC there is a dense disk of dust.

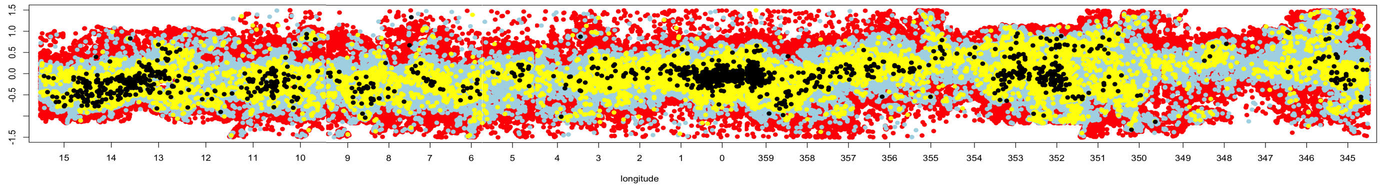

Fig. 3. Longitude-latitude plot of all GLIMPSE stars with $Ak > 1.0$ in a narrow strip along the Galactic equator ($-15° < l < +15°$ and $-1.5° < b < +1.5°$). Each star is colored according to its Ak value: $Ak > 1.0$(red); >1.5 (light blue); >2.0 (yellow); >2.5 (black).

Figure 3 offers another view on the distribution of dust in the Galactic plane between $|b| \leq 1.5°$ and between $l = \pm 15°$ from the GC. It shows the longitude-latitude locations of all GLIMPSE stars for which Ak could be determined. Each dot is colored according to the stellar Ak value. The dust disk has (on average) a constant thickness, with $-1° < b < +1°$ for the red points, a somewhat reduced thickness for the light blue objects ($Ak > 1.5$), and a still thinner layer for the yellow points. The yellow points ($Ak > 2.0$) are found in large areas but their distribution is not uniform over the full longitude range. The black points ($Ak > 2.5$) are rare and in most places they are isolated objects except near $l = 0°$. There we see the Nuclear Stellar Disk (NSD). Fig. 3 shows that the NSD is embedded in the dust layer.

One more conclusion can be drawn from Fig. 3: the distribution in latitude of the yellow points is a factor of two to three smaller than that of the red points. Assuming that the red and the yellow stars have the same z distribution (i.e. perpendicular to the Galactic plane) the yellow stars must be about two or three times farther away as the red stars. They may be at the far end of the AGB disk as seen from our position.

Several recent papers show diagrams similar to Fig. 3: Simion et al. (2017) Fig. 1; Soto et al. (2019), Fig. 2; Surot et al. (2020), Fig. 3. Our results compare very well; our data are more limited in latitude but at least one magnitude deeper in Ak.

3. Counting the stars, matrix Rml

We counted the stars in 51 fields along the Galactic equator, each of size $\Delta l \times \Delta b = 1° \times 3°$, in magnitude between [8.0] = 3.5 and 11.5 using $\Delta[8.0] = 1.0$. The result is a matrix Nml. In paper I, we discussed the exponential increase in numbers with magnitude, always with the same rate of growth. To make numbers at different magnitudes comparable we used $Rml = 10^{-0.4 \cdot [8.0]} \cdot Nml$.

A general conclusion is that for magnitudes [8.0] > 6.5 plots of the columns of Rml are qualitatively very similar. This is illustrated in Fig. 4 where the values of Rml at [8.0] = 8.25 are shown in the y-direction; in the x-direction the Rml values for [8.0] = 10.25. The ratio of x to y is the same in all longitude directions except for two points at the top of the diagram that correspond to the directions $l = -1°$ and 0°. This qualitative similarity has been an argument to assume that different columns of Rml (and of Nml) have a very similar underlying structure. A relatively simple model for the density, $\rho(R)$, and for the luminosity distribution, $\Psi(L)$, might explain the distribution of the numbers in the Rml matrix.

3.1. Two different populations and a third in the NSD

Fig. 5 (top) shows the number of all AGB stars with [8.0] < 12.0 in relation to longitude. We see a broad base from $l = -60°$ to $l = +60°$ and between $l = \pm 10°$ a narrow peak above the base.

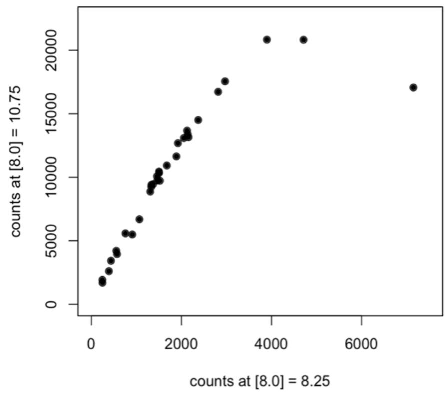

Fig. 4. In the horizontal direction Rml values at [8.0] = 7.5 and in the vertical direction those at [8.0] = 10.75 at all longitudes of the inner disk. The ratio of the two is approximately constant, except for the points representing $l = 0°$ and $l = -1°$.

Similar plots at different values of [8.0] are qualitatively very similar, except for [8.0] < 6.0; there the narrow peak is missing and only the broad base remains (see the bottom diagram in Fig. 5). Two populations are thus involved. First, the broad rather flat outer disk. Second, the inner disk that produces the sharp peak. Both distributions are thin in the z direction, as may be seen in Fig. 3. There is a third population in the innermost part of the disk, for $R < 0.2$ kpc. A first indication is the isolated high point in Figure 5 in the direction $l = 0°$.

We searched the existing literature for another mention of the inner disk and did not find any, except in a paper by Natale et al. (2022). These authors find, unexpectedly, a thin inner disk. It might be the same as our inner disk but theirs has a radius of 4.5 kpc and ours of 1.42 kpc ($= R_{GC} \cdot \sin(10°)$).

The inner disk clearly lacks stars brighter than [8.0] = 6.5; what is the significance of this conclusion? In paper I, we concluded that in long-period variables (LPVs) a shorter pulsation period implies a lower maximum luminosity and as these stars are of somewhat lower mass, this implies that AGB stars of lower stellar mass reach a lower maximum luminosity. Is this argument valid and do the stars of the inner disk have a somewhat lower mass? Contradicting this is the fact that the distribution of OH/IR stars along the Galactic plane does not show a discontinuity in stellar properties at $l = \pm 10°$, except in the kinematics, as we mention below.

3.2. Model density distribution of the AGB stars in the plane of the Milky Way

The peak in Fig. 5 shows a steep increase in number toward the GC. This resembles the steep increase in numbers when one enters a globular cluster, and that led us to describe the increase in density with a toy model for globular clusters, a

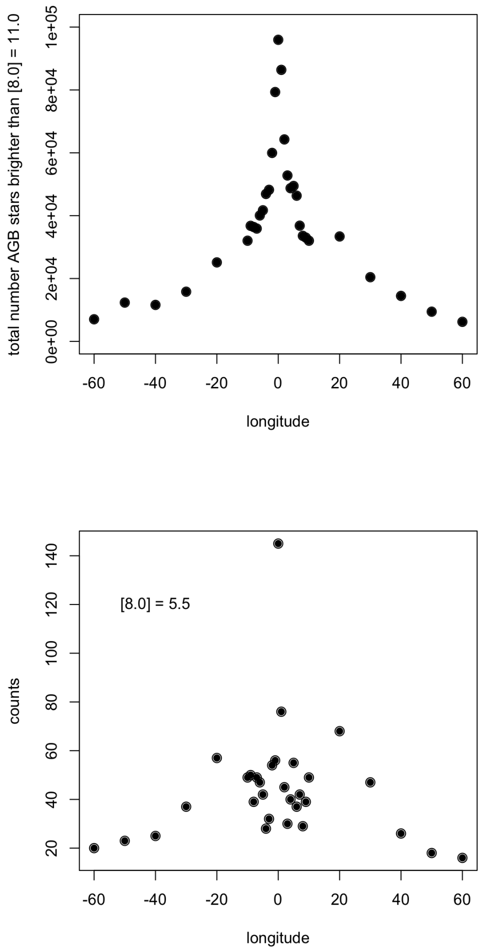

Fig. 5. Counts of stars within an area of one square degree in fields at all available longitudes. Top: for [8.0] < 12.0; Bottom: for [8.0] = 5. In the bottom diagram there is a single isolated point at $Rml \approx 140$ and $l = 0°$; it represents the NSD.

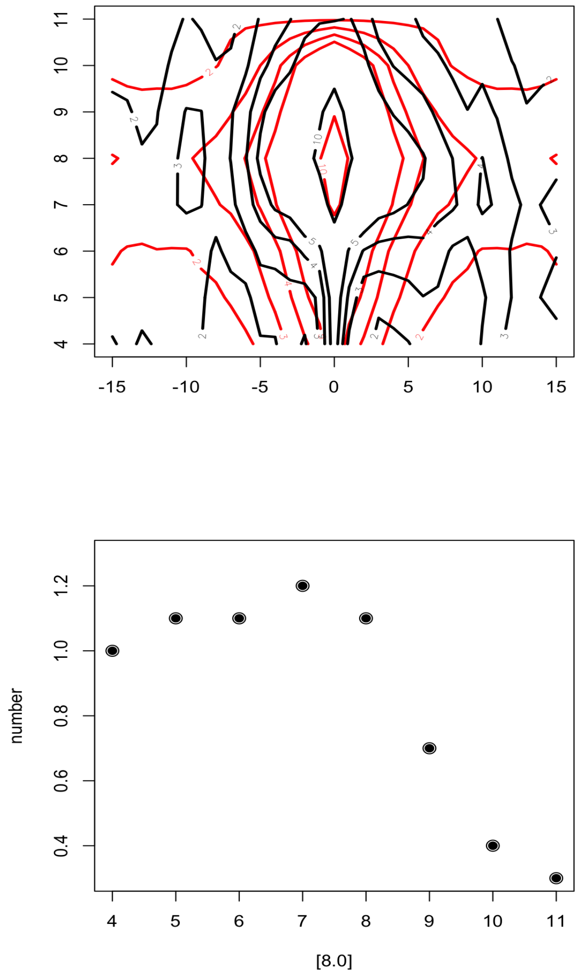

Fig. 6. Top: in red the contour diagram of the chosen model distribution in longitude and apparent magnitude; in black the observations (matrix *Rml*); bottom: the adopted distribution in apparent magnitudes [8.0]. To obtain the absolute magnitudes of these stars, subtract 14.56.

Plummer function (Plummer 1911; Dejonghe 1984). The function describes the steep frontiers of globular clusters but it has a flat circular top.

The stellar density in the outer disk is described by an exponential relation, $\rho(R) \propto e^{-R/Rh}$, where R is the distance to the GC and Rh is a scale length of about 3.5–4 kpc. This confirms conclusions derived in other, older studies – see e.g. Robitaille et al. (2012).

In addition we assume a third population within 300 pc from the GC.

This leads to the following set of equations for ρ, the stellar density:

(1) Galactic center. $\rho = 2 \cdot A/a^2$ for $R < 0.3$ kpc

(2) Inner disk. $\rho = \frac{A \cdot a^2}{(a^2+R^2)^2}$ for $0.2\,\mathrm{kpc} \leq R \leq 1.4$kpc

(3) Outer disk. $\rho = D \cdot e^{-R/Rh}$, for $R > 1.4$ kpc

The chosen values of A, D, a and Rh (10, 4.5, 0.7, 3.5), establish the structure of the building assigned to the AGB stars, a building measured in size by the distance modulus, $\mu = m - M$. To select the inhabitants, the population of the AGB stars, we need the distribution of their absolute magnitudes, $\Psi(M)$. Figure 7 gives us confidence that all stars within 10° from the GC have almost the same distance ($\mu = m - M = 14.56$) and thus we define the population by the distribution of the apparent magnitudes $\psi([8.0])$; see the bottom diagram of Fig. 6.

This brings us to the contour diagram in Fig. 6. The black lines present the observations and the red lines the selected model. We conclude that the observations are well described by the model. A significant detail in the observations is the ridge toward brighter magnitudes near $l = 0°$. It is caused by the exceptional population near the GC, in particular by the NSD.

With this mathematical model we calculated the density distribution, ρ, of the stars along a given line of sight, l. Figure 7 shows that in all longitude directions, except those far away from the GC, the density of the AGB stars has a strong maximum at the sub-central point, i.e. at the galactocentric distance $R_{GC} \cdot \cos(l)$.

3.3. Location of the bar?

At the beginning of this study we expected to find strong evidence for the Galactic bar but we did not find any. Related work by Iwanek et al. (2023) helped to understand our failure. Their Fig. 4 shows that the effects of the bar become visible in the faintest contours, far away at negative longitudes and nearby at positive longitudes. The authors separate stars near and far by the pulsation period. That information is missing in our data and therefore we do not see the bar. The symmetry around the rotation axis of the Milky Way explains our counts sufficiently; there

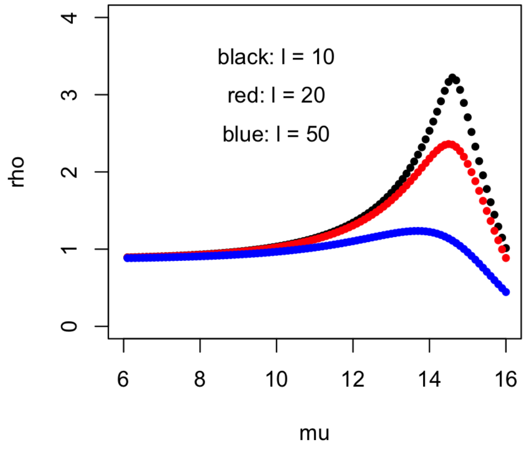

Fig. 7. Density of AGB stars, *Rml*, along the line of sight in the directions $l = 10°$, $l = 20°$, $l = 50°$ calculated as a function of distance $\mu = m - M$.

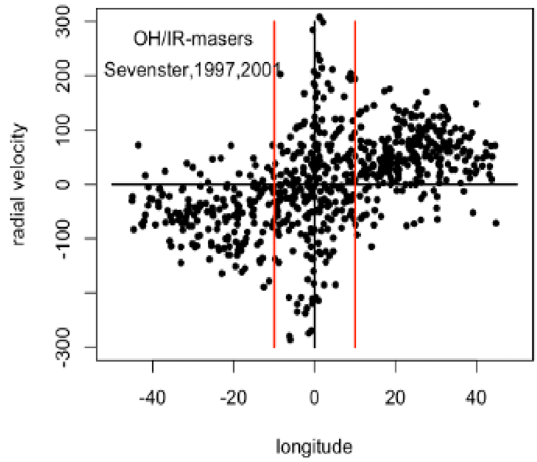

Fig. 8. Stellar velocities of OH/IR maser stars by Sevenster (see text for references). The two red vertical lines separate the inner and outer disks. The radial velocity distribution is different between the two samples.

is no need for a bar. Our observations do not reject the existence of the bar, nor do they confirm it.

In their early analysis of the GLIMPSE data Benjamin et al. (2005) find indications for the existence of the bar in stars with $11.5 < [8.0] < 13.5$. We excluded those faint objects from our study.

3.4. Kinematics

The longitude distribution of OH maser stars, which are AGB stars par excellence, does not show a discontinuity at longitude $l = \pm 10°$, the separation between inner and outer disk. However, there is a discontinuity in the kinematics. Figure 8 is based on the systematic searches by Sevenster et al. (1997a), Sevenster et al. (1997b), Sevenster et al. (2001). In the outer disk, $l > 10°$ and $l < -10°$, the stars follow Galactic rotation: positive velocities for $l > 10°$ and negative velocities for $l < -10°$. In the inner disk the average radial velocity drops toward the GC and ever more stars have a forbidden velocity ($l > 0°$, $V < 0$ and $l < 0°$, $V > 0$); the average radial velocity decreases to zero when one approaches the GC. The population of the inner disk is kinetically different from that of the outer disk.

4. The inner few degrees: the inner galactic bulge (IGB) and the nuclear stellar disk (NSD)

The first detection of Galactic center stars was achieved at 2.2 μm (Becklin & Neugebauer 1968). The distribution of the stars within a few degrees has since been the subject of many studies. From observations at near-IR wavelengths Catchpole et al. (1990) found a strongly elliptical (l, b) distribution in the inner few arcminutes. In 1983 IRAS made almost complete IR maps of the full sky, including the inner Milky Way. Insufficient angular resolution prevented an accurate description of the stellar distribution inside one degree from the GC. ISO has given interesting results on the IR-properties of stars in the Galactic bulge, but not a full overview (see Perault et al. 1996; Ojha et al. 2003). The MSX-surveys provided more information (Ojha et al. 2007) but their sensitivity was limited and the full picture remained hidden. The GLIMPSE-database offers an overview of the distribution of AGB stars within a few hundred parsecs around the GC; the GLIMPSE data are constrained by sensitivity and confusion but enough information is left to give the desired description.

4.1. The inner Galactic bulge, IGB

In the 1930s the first realistic models were made of the stellar distribution in the Milky Way. A book by de Sitter (1932) contains a profile (drawn by J. H. Oort) of our Galaxy that already shows a prominent bulge. Numerous optical observations and analyses have been made of the Galactic bulge but severe interstellar extinction prevented the detection of stars within a few degrees from the Galactic equator.

A prominent bulge with a size of $10° \times 4°$ is present in the data of COBE (see e.g. Jönsson et al. 2017) but does not reach the inner few degrees. The GLIMPSE database provides this missing information. Our discussion will be limited to these inner few degrees around the GC and does not concern the large scale structure of the bulge as described by Wegg & Gerhard (2013) and Ness & Lang (2016).

The GLIMPSE survey is limited in Galactic latitude, $|b| \leq 1.5°$, but around the GC higher latitudes have also been covered. Figure 9 shows two contour diagrams of the number density of stars. The top diagram contains the *lb* plot of the long-period variables detected in the OGLE survey (Iwanek et al. 2022, Iwanek et al. 2023). The bottom diagram is a contour diagram of the AGB stars brighter than $[8.0] = 11.0$ out to $b = \pm 4°$. Long-period variables are AGB stars and thus these two diagrams are complementary.

Unfortunately, the GLIMPSE database contains erroneous objects, marked by the two broken lines parallel to the Galactic equator. Confirmation that these objects are false is their absence in the upper figure.

Asymptotic Giant Branch stars are stars of modest mass (1–4 M_{sun}) and thus we see, for the first time, the distribution of such stars in the immediate surroundings of the GC, in the innermost part of our Milky Way. It emphasizes how much is gained by studying stars at the wavelengths where interstellar extinction is very low and the stars are at their brightest.

Figure 10 shows the outermost contours of the IGB and at its center the much smaller NSD (in red), which we discuss next.

4.2. The nuclear stellar disk, NSD

The NSD at the center of our Milky Way is a disk of stars and dust. In 1990 Catchpole et al. (1990) used near-IR measurements and saw that the stars formed an elliptical distribution around

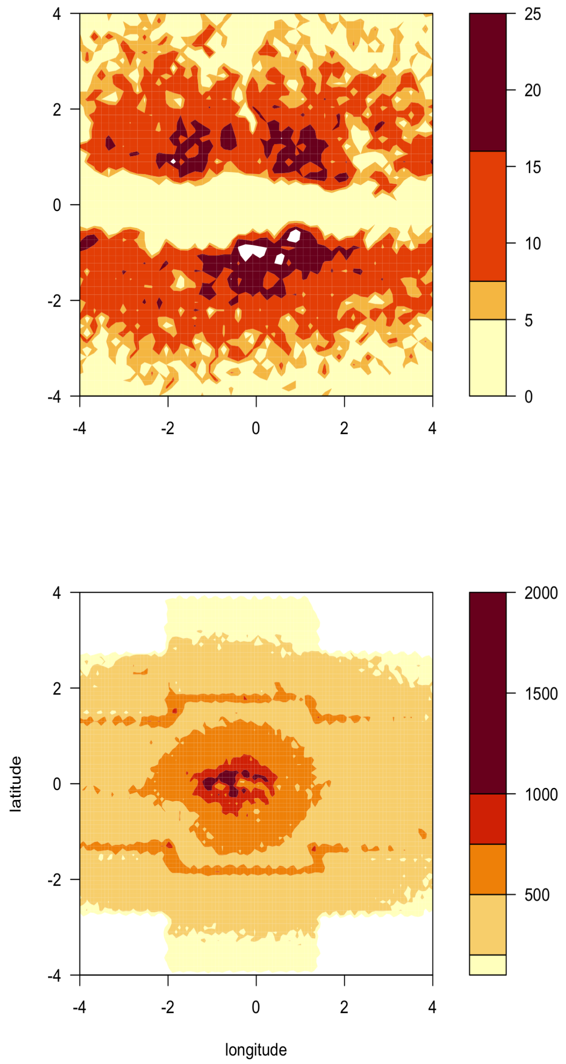

Fig. 9. Contour diagrams in longitude and latitude of the number of stars counted within squares of $0.1^\circ \times 0.1^\circ$. Top: distribution of Miras (long-period variables) detected in the OGLE survey (Iwanek et al. 2023). Bottom: Distribution of GLIMPSE AGB stars. The two red lines indicate a range of false sources (see text). Baade's window is at $(l, b) = (1.02, -3.92)$ and has a size of about 1 square degree.

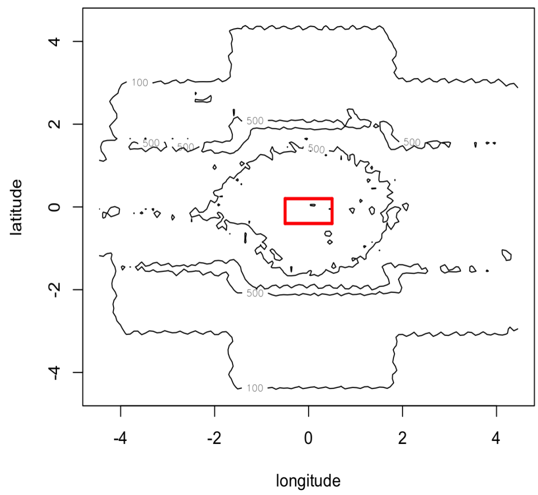

Fig. 10. Schematic contour diagram to illustrate the locations of the IGB and of the NSD (in red). The two objects are very different in size

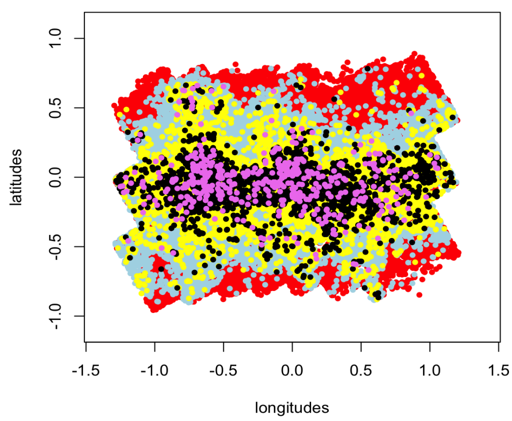

Fig. 11. Longitude-latitude plot of 36 500 stars with [8.0] < 8.5 from the SSTGC version of the GLIMPSE database. The color of the points corresponds to the value of Ak. Ak > 1.0 (red); Ak > 1.5 (light blue); Ak > 2.0 (yellow); Ak > 2.5 (black); Ak > 3.0 (violet).

the Galactic Center even down to the innermost arc minutes. Lindqvist et al. (1992b) detected OH-masers within arcminutes from the GC and Lindqvist et al. (1992a) found net rotation in the sample. Launhardt et al. (2002) combined radio measurements of interstellar gas and an infrared map by COBE and argued that there is a coherent structure forming a discrete object that they called the nuclear stellar disk. They gave it a size of 460×90 pc and mention the presence of a warmer inner disk with a length of 220 pc.

Similar disks have been seen in other galaxies. They are thought to have been formed when interstellar gas flowed to the center of the galaxy during the formation of a bar. Many studies of our own NSD have been made, but we do not discuss them here. Our goal is limited; we show the prominent presence of the NSD in the GLIMPSE AGB stars and expect that that offers opportunities for more detailed studies. A few recent papers on the NSD are Sanders et al. (2024), Prudil et al. (2025) and Feldmeier-Krause et al. (2025). For further study we refer to these papers.

Figure 11 shows 36 600 point sources from the SSTGC catalog brighter than [8.0] < 8.5; the NSD is the outstanding feature.

To measure the size of the NSD we counted the number of stars in two narrow, orthogonal strips with a width of 15 pc, one in the longitude direction and the other in the latitude direction (see Fig. 12). The diagrams show that the NSD has sharp limits of $-0.5^\circ < l < 0.5^\circ$ and $-0.3^\circ < b < 0.2^\circ$. These limits are significantly smaller than assumed by Nishiyama et al. (2013), for example. Our boundaries correspond to the rectangle in Fig. 7 in Gallego-Cano et al. (2020), which is small compared to their overall map. This smaller outline is also seen in the contour map based on Mira variables by Sanders et al. (2024).

The two narrow strips show that the NSD is a separate object on the peak of the inner disk. This supports the conclusion from spectroscopy of massive stars (Schultheis et al. 2021) that the NSD is an object of its own, not the peak of the inner disk; the NSD is the plum on the pudding: right in the middle but an element of its own.

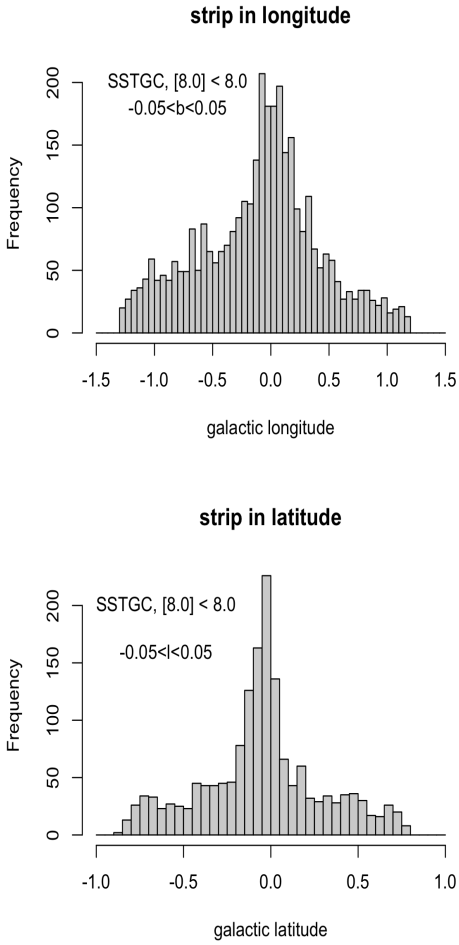

Fig. 12. Histograms of the number of stars along a strip of width 0.1° (15 pc) through the GC. The top strip is in the direction of longitude, the other in the direction of latitude. The NSD is marked by a sharp and large increase in numbers.

4.3. The nature of the objects within the NSD limits

The stars in the NSD are surprisingly bright. Are they AGB stars? We determined their color $K - [8.0]$ before and after correction for interstellar extinction. The distribution of this color was narrow but not as narrow as in Fig. 7 in paper I.

We selected 1648 stars within the positional limit of the NSD and with $Ak > 2.5$. We determined their apparent bolometric magnitude, $m_{bol} = 10.55 + dmag$ (see paper I) and used $(m - M) = 14.5$ to obtain $M_{bol} = dmag - 4.05$. Fig. 13 shows the histogram of M_{bol}. The colors and the values of M_{bol} are not precisely those found before but close enough to identify them as AGB stars.

4.4. The three bright clusters in the NSD

The NSD contains three well-known star clusters, the Arches, the Quintuplet and the SgrA cluster. Figure 14 shows objects with $[8.0] < 6.0$ from the SSTGC database. The red dots represent the three well-known clusters within the NSD: from left to right: the SgrA cluster, the Arches cluster and the Quintuplet cluster. Three GLIMPSE objects coincide to within 2″ with known Quintuplet stars, notably the "Pistol"-star and two supergiants. The SgrA cluster and the Quintuplet cluster coincide with a concentration of bright SSTGC-stars, but there is no sign of the Arches cluster.

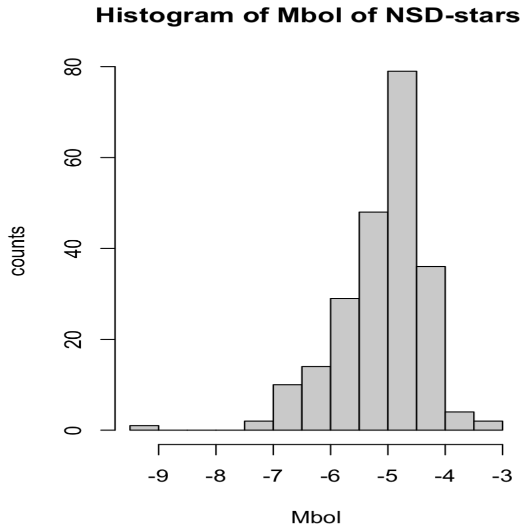

Fig. 13. Histogram of the bolometric magnitudes of AGB stars in the NSD with extinction $Ak > 2.5$.

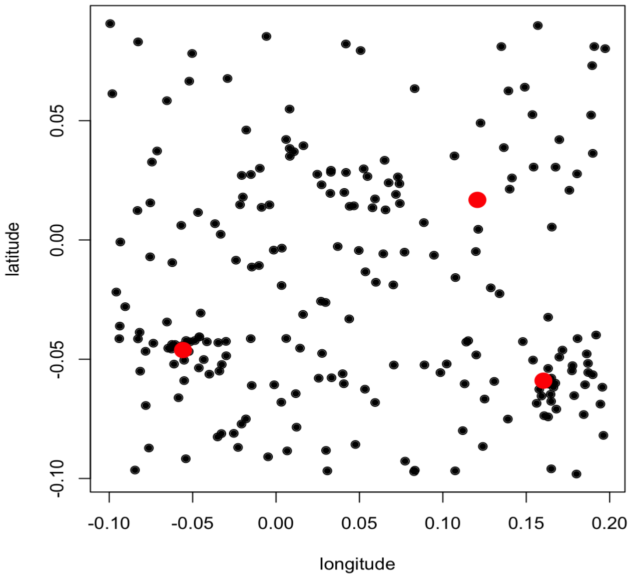

Fig. 14. Distribution of bright SSTGC stars ($[8.0] < 6.0$). The three red dots indicate the central positions of (from left to right) the Sgr A , the Arches and the Quintuplet cluster.

Using isochrones by Marigo et al. (2008) we conclude that the cluster must be younger than 60 Myr to not contain an AGB star.

5. Conclusions

The main conclusions in this paper are as follows:

1. The extinction values of the AGB stars show that they form a flat, circular disk with a radius of 7 kpc. This disk of stars is embedded in a dust disk that, on a Galactic scale, is of uniform density. Within a few hundred parsecs from the GC the stars are embedded in a separate, thicker dust disk;
2. The stellar distribution in longitude is axially symmetric around the GC. There is an *outer disk* stretching from R = 1.4 kpc to larger distances; its stellar density varies as $e^{-R/Rh}$. Inside $l = \pm 10°$, or $R \leq 1.4$ kpc, an *inner disk* appears with a sharply defined boundary and a very steep increase in numbers when one moves toward the GC. Within some 200 pc

there is third population that contains the inner Galactic bulge (IGB) and the Nuclear Stellar Disk (NSD);
3. Along a line of sight in direction l the distribution of stars is strongly concentrated around the sub-central distance ($R_{GC} \cdot \cos(l)$). This explains why CMDs of apparent magnitudes resemble CMDs of absolute magnitudes;
4. Within 4° from the GC the IGB is easily recognized in the distribution of AGB stars brighter than $[8.0] < 11.0$;
5. Within 1.5° (≈200 pc) from the GC the rotating NSD is a dominant feature in (l, b)-maps. Its stars have a very strong extinction ($Ak > 2.5$ or $Av > 25$). The NSD is an object of its own and it is independent of the inner disk;
6. Inside the NSD the Sagittarius A cluster and the Quintuplet cluster contain AGB stars but the Arches cluster does not: it apparently is too young to have produced them.

References

Becklin, E., & Neugebauer, G. 1968, ApJ, 151, 145
Benjamin, R., Churchwell, E., Babler, B., et al. 2005, ApJ, 630, L149
Catchpole, R., Whitelock, R., & Glass, I. 1990, MNRAS, 247, 479
Churchwell, E., Babler, B. L., Meade, M. R., et al. 2009, PASP, 121, 213
de Sitter, W. 1932, "Kosmos", (reprint 2009, Amsterdam University Press)
Dame, T. M., Hartmann, D., & Thaddeus, P. 2001, ApJ, 547, 792
Dejonghe, H. 1984, A&A, 133, 250
Feldmeier-Krause, A., Neumayer, N., Seth, A., et al. 2025, A&A, 696, A213
Gallego-Cano, E., Schödel, R., Nogueras-Lara, F., et al. 2020, A&A, 634, A71
Güver, T., & Özel, F. 2009, MNRAS, 400, 2050
Iwanek, P., Soszyński, I., Kozłowski, S., et al. 2022, ApJS, 260, 46
Iwanek, P., Poleski, R., Kozłowski, S., et al. 2023, ApJS, 264, 20
Jönsson, H., Ryde, N., Schultheis, M., & Zoccali, M. 2017, A&A, 598, A101
Launhardt, R., Zylka, R., & Mezger, P. 2002, A&A, 384, 112
Lindqvist, M., Habing, H., & Winnberg, A. 1992a, A&A, 259, 118
Lindqvist, M., Winnberg, A., Habing, H., & Matthews, A. 1992b, A&AS, 92, 43
Majewski, S. R., Zasowski, G., & Nidever, D. L. 2011, ApJ, 739, 25
Marigo, P., Girardi, L., Bressan, A., et al. 2008, A&A, 482, 883
Natale, G., Popescu, C., Rushton, M., et al. 2022, MNRAS, 509, 2339
Ness, M., & Lang, D. 2016, AJ, 152, 14
Nishiyama, S., Kazuki, Y., Tetsuya, N., et al. 2013, ApJ, 769, L28
Ojha, D. K., Omont, A., Schuller, F., et al. 2003, A&A, 403, 141
Ojha, D. K., Tej, A., Schultheis, M., Omont, A., & Schuller, F. 2007, MNRAS, 381, 1219
Perault, M., Omont, A., Simon, G., et al. 1996, A&A, 315, L165
Plummer, H. 1911, MNRAS, 71, 460
Prudil, Z., Kunder, A., Beraldo e Silva, L., et al. 2025, A&A, 695, A211
Reid, M. J., Menten, K. M., Brunthaler, A., et al. 2019, ApJ, 885, 131
Robitaille, T. P., Churchwell, E., Benjamin, R. A., et al. 2012, A&A, 545, A39
Robitaille, T. P., Meade, M. R., Babler, B. L., et al. 2008, AJ, 136, 2413
Sanders, J., Kawata, D., Matsunaga, N., et al. 2024, MNRAS, 530, 2972
Schultheis, M., Fritz, T. K., Nandakumar, G., et al. 2021, A&A, 650, A191
Sevenster, M. N., Chapman, J. M., Habing, H. J., Killeen, N. E. B., & Lindqvist, M. 1997a, A&AS, 122, 79
Sevenster, M. N., Chapman, J. M., Habing, H. J., Killeen, N. E. B., & Lindqvist, M. 1997b, A&AS, 124, 509
Sevenster, M. N., van Langevelde, H. J., Moody, R. A., et al. 2001, A&A, 366, 481
Simion, I. T., Belokurov, V., Irwin, M., et al. 2017, MNRAS, 471, 4323
Soto, M., Barbá, R., Minniti, D., et al. 2019, MNRAS, 488, 2650
Surot, F., Valenti, E., Gonzalez, O. A., et al. 2020, A&A, 644, A140
Vergely, J., Lallement, R., & Cox, N. 2022, A&A, 664, A174
Wegg, C., & Gerhard, O. 2013, MNRAS, 435, 1874
Zhang, M., Kainulainen, J., Zhao, H., et al. 2025, MNRAS, 543, 3830